Photo-excited Toluidine Blue inhibits full-length Tau aggregation in Alzheimer' disease

Tushar Dubey [1, 2], Nalini Vijay Gorantla [1, 2] Kagepura Thammaiah Chandrashekara [3], Subashchandrabose Chinnathambi [1, 2*]

[1]Neurobiology Group, Division of Biochemical Sciences, CSIR-National Chemical Laboratory, Dr. Homi Bhabha Road, 411008 Pune, India
[2]Academy of Scientific and Innovative Research (AcSIR), 411008 Pune, India
[3]Institution of Excellence, Vijnana Bhavan, University of Mysore, Manasagangotri, 570006 Mysore, India

[*] To whom correspondence should be addressed**: Prof. Subashchandrabose Chinnathambi**, Neurobiology group, Division of Biochemical Sciences, CSIR-National Chemical Laboratory (CSIR-NCL), Dr. Homi Bhabha Road, 411008 Pune, India, Telephone: +91-20-25902232, Fax. +91-20-25902648. Email: s.chinnathambi@ncl.res.in

ABSTRACT

The aggregates of microtubule-associated protein Tau are the major hallmark of Alzheimer's disease. Tau aggregates accumulate intracellularly thus leading to generation of neuronal toxicity. Numerous approaches have been targeted against Tau protein aggregation, which include application of synthetic and natural compounds. Toluidine blue is a basic dye of phenothiazine family, which irradiation with 630 nm light converted to photo-excited form leading to generation of singlet oxygen species. In present work we studied the potency of Toluidine blue and photo-excited Toluidine blue against Tau aggregation. Biochemical and biophysical analysis using ThS fluorescence, SDS-PAGE, CD spectroscopy and electron microscopy suggested that Toluidine blue inhibits the aggregation of Tau *in-vitro*. The Photo-excited toluidine blue potentially dissolved the matured Tau fibrils, which was indicating disaggregation property of Toluidine blue. The cell biology studies including cytotoxicity assays, ROS production assays suggested Toluidine blue to be a biocompatible dye as reduced ROS levels and cytotoxicity was observed after exposure of Toluidine blue on Tau stressed cells. The photo-excited Toluidine blue modulates the cytoskeleton network in cells, which was supported by immunofluorescence studies of neuronal cells. The studies in UAS Tau E14 transgenic Drosophila model suggested that photo-excited Toluidine blue was potent to restore the survival and memory deficit of Drosophila. The overall findings of our studies suggests that Toluidine blue to be a potent molecule in rescuing the Tau-mediated pathology by inhibiting its aggregation, reducing the cytotoxicity; modulating the tubulin level and behavioral characteristics of Drosophila. Thus Toluidine blue can be addressed as a potent molecule against Alzheimer's disease.

Keywords

Alzheimer's disease, Tau, Toluidine Blue, Photo-excitation, ROS production, UAS Tau E14 transgenic Drosophila.

INTRODUCTION

Alzheimer's disease (AD) is a progressive neurodegenerative disorder characterized by decline in the cognitive function, inefficacy to perform regular work along with social withdrawal and poor judgment. AD is associated with short-term memory loss, which predominantly affects CA1, CA3 and Dentate gyrus regions of hippocampus. Extracellular senile plaques composed of Amyloid-β (Aβ) and intracellular neurofibrillary tangles (NFTs) are the known causes of AD [1-4]. The physiological role of Tau is to stabilize the microtubules. In pathological conditions, Tau undergoes various post-translational modifications, oxidative stress and truncation resulting in its aggregation[5-8]. These aggregates are emerging as new targets for screening small molecules, leading to the path of drug discovery in AD[5]. Small molecules of natural and synthetic origin were being studied extensively for their medicinal potency against AD pathology[3, 6, 7]. Research led to identification of different classes of dyes such as phenothiazine, xanthine *etc.* that initially showed therapeutic potency in AD. Methylene blue (MB) and its derivative were found to be more potent against AD [9]. MB is known as methylthioninium and exists in equilibrium with its reduced form *i.e.,* leucomethylthioninium (LMT). Addition of two extra methyl groups forms dimethyl-MTC (DMMTC); and sulphur and bromine forms dihydromesylate and dihydrobromide form of LMT respectively. Harrington *et al.,* studied different forms of MB to understand the mechanism of Tau aggregation during its degradation in template-dependent manner. The mono- and di-demethylated metabolites of MB yield Azure A and Azure B respectively. MB exists in both inactive oxidized forma and active reduced form. These metabolites inhibit Tau aggregation by involving in redox cycles of two cysteine residues in third and fourth repeat; and thus maintaining Tau in its native conformation[10]. Furthermore, the cysteine residues were modified to sulfenic, sulfinic and sulfonic acid, which convert Tau to aggregation incompetent form. Unlike the parent moiety of MB, which interacts with cysteine residues, Azure A and Azure B shows interaction with aromatic amino acids, thereby preventing Tau aggregation. For its mechanism of action Azure A prefers β-sheet conformation of Tau[11]. MB modifies the deprotonated sulphur at Cys163 in the catalytic domain by sulfenation, thus inhibiting and reducing the truncation and aggregation of Tau respectively[12]. MB inhibits oligomer formation in Amyloid-β, which are more toxic and accelerate the less toxic fibril formation. HT-22 cells were used to study the role of oxidized and reduced form of MB in neurodegenerative disorders [13]. Among them, compounds containing phenothiazine nucleus alone and its derivatives of MB and TB showed neuroprotective properties and decreased singlet oxygen production. *Drosophila* AD model explained the significance of photosensitized MB on Amyloid-β disaggregation. Drosophila genome shares conserved neurological, developmental, and physiological properties with human genome, hence *Drosophila* is an important system to study the human neurodegenerative diseases and would be ideal for *in vivo* testing and screening of therapeutic molecules[14 15]. Photodynamic therapy (PDT) is widely used for the treatment of carcinomas, biofilms, dental plaques, and dermatological problems *etc*. Photo-excited TB is widely used as bactericide, but its effect in neuronal degeneration is yet to be addressed. Principally, the therapy is based on targeting disaggregation potency of photo-excited dyes against pathological protein aggregates. PDT was found to be effective in inhibiting Amyloid-β aggregation and increasing its disaggregation by employing xanthene and porphyrin dyes. TB has been reported for its inhibition properties against proteins like prion, Amyloid-β and Tau *etc.*[16-18]. The aim of present work was to study the potency of TB and PE-TB against Tau aggregation and toxicity. The hypothesis was evaluated by using the biochemical and biophysical assays-like ThS fluorescence assay, SDS-PAGE, TEM and CD spectroscopy. The biocompatibility of TB and PE-TB was tested in neuroblastoma cells and Transgenic *Drosophila* model. The fruit fly (*Drosophila melanogaster*) is a supermodel having about 74% of genetically resemblance with human genes, and is being used as a model organism to study the neurodegenerative diseases-like Tauopathy and AD. Drosophila has similar organization of brain as human where Tau plays critical role in maintaining the integrity of

cytoskeleton of neuron. The mutation in Tau protein in Drosophila brain leads to formation of NFTs which, mimics the Tauopathy condition of human brain.[19]. The overall *in vitro* and *in vivo* studies indicate the potency of TB and photo-excited TB in rescuing the Tau aggregation mediated toxicity. The studies including cytotoxicity, cognitive impairment and generation of ROS, ultimately suggested the potency of TB against Alzheimer's-related pathology.

MATERIALS AND METHODS

Chemicals and reagents

MES, Heparin, BES, BCA, $CuSO_4$, ThS, ANS, DNPH, Toluidine Blue, MTT and DMSO were purchased from Sigma. IPTG and DTT were purchased from Calbiochem. Other chemicals such as ampicillin, NaCl, KCl, Na_2HPO_4, KH_2PO_4, EGTA, $MgCl_2$, PMSF, ammonium acetate and BSA were from MP and protease inhibitor cocktail was from Roche. Copper coated carbon grids were purchased from Ted Pella, Inc. Advanced DMEM/F-12 media, fetal bovine serum (FBS), pensterp cocktail, anti-anti were purchased from Gibco. All laboratory reagents used for *Drosophila* studies were purchased from Merck, unless otherwise mentioned.

Recombinant preparation of Tau

The recombinant full-length Tau were expressed in *E. coli* BL21* strain. The cells were grown at 37°C till the OD_{600} reached to 0.5 to 0.6. It was then induced with 0.5 mM IPTG and was further incubated for 4 hours and harvested by centrifugation at 4000 rpm for 10 minutes. The protein isolation and purification was done as described previously[20]. The lysing of cells was done using homogenizer Constant Cell Disruption systems. The cells were resuspended in Buffer A composed of 50 mM MES, 1 mM EGTA, 2 mM $MgCl_2$, 5 mM DTT, 1 mM PMSF and 50 mM NaCl and was subjected to homogenization at 15,000 psi pressure. The obtained lysate was heated at 90°C for 20 minutes in presence of 0.5 M NaCl and 5 mM DTT. This was cooled and centrifuged at 40,000 rpm for 45 minutes. The supernatant was collected and dialyzed overnight against Buffer A before loading to cation exchange column. Increasing the ionic gradient of NaCl to 1 M eluted tau protein. The protein quality was analyzed by SDS-PAGE and further passed through size exclusion chromatography. The obtained protein was analyzed, pooled and concentrated. The concentration was estimated by BCA assay and stored at -80°C till further used. Tau aggregation was induced at 37°C with heparin as previously described[21]. Tau in presence of anionic inducer such as heparin, RNA, arachidonic acid *etc.* undergoes aggregation. Among all these molecules heparin induced Tau aggregation is widely accepted model for *in vitro* Tauopathy studies. Earlier studies suggested the heparin mediated Tau aggregation followed the heparin induced Tau aggregation model to demonstrate the transition of Tau from random coil to β-sheets upon aggregation [22]. Taniguchi *et al.* demonstrate the inhibition of heparin induced Tau filaments by phenothiazine, polyphenols and porphyrins [11]. In present work we used heparin induced Tau aggregation, the soluble full-length Tau was mixed with heparin (17,500 Da) at a ratio of 4:1. The reaction was carried out in 20 mM BES buffer supplemented with 25 mM NaCl, 1 mM DTT, 0.01% NaN_3 and protease inhibitor cocktail mixtures.

Thioflavin S Fluorescence Assay

The effect of TB on aggregation property of Tau was measured by Thioflavin S (ThS) fluorescence assay. ThS is a mixture of methylated dehydrothiotoluidine and sulfonic acid, has property to fluorescence on binding to β-sheet structures. In present assay, the protocol of ThS assay was followed as described by Santa-Maria *et al.*[23]. The fluorescence measurement was carried out by

incubating 2 µM of Tau with ThS in 1:4 ratios for 15 minutes in dark. All the reaction mixtures were measured in triplicate in TECAN Infinite M200 pro spectrophotometer at an excitation of 440 nm and emission of 521 nm. Further, the data was analyzed using Sigma Plot 10.0.

Circular Dichroism Spectroscopy

The conformational changes in Tau were analyzed by using CD spectroscopy in far-UV region. In native conditions Tau has typical random coil conformation, but the aggregation causes conformational change to β-sheet, which absorbs around 220 nm. The effect of TB on conformational changes in Tau was studied as described previously[24]. All the spectra were measured in Jasco J-815 spectrometer by diluting full-length Tau to 3 µM in 50 mM phosphate buffer at pH 6.8.

Binding Constant

Binding constant of TB with Tau was estimated by UV-visible spectroscopy. The experiment was performed using 96 well clear bottom plate (Eppendorf) and measurements were recorded in Tecan Infinite M200 PRO spectrophotometer. 20 µM of TB was incubated with varying concentrations of Tau (0, 10, 20, 30, 40, 50 µM). Binding constant (K_D) value was calculated after recording the spectrum from 230 to 800 nm. The absorption maximum of Tau was observed at 314 nm. All the samples were diluted in phosphate buffer, at pH 6.8.

$$[PL] = \frac{[P_o] \times [L]}{K_D + [L]}$$

Here, $[P_o]$ is initial protein concentration, [L] is free ligand concentration, [PL] is concentration of protein-ligand complex and K_D is dissociation constant.

Light-induced Inhibition of Tau Assembly

For analyzing the effect of photo-excited TB on Tau aggregates, aggregates were incubated for one hour in dark with varying concentration of TB (2, 5, 10, 20 and 40 µM). 200 µL of reaction mixture was added in 96 black well plate (Eppendorf) and was irradiated in dark using red LED. For PDT experiments, three controls were considered; dark control (DC) containing TB treated Tau aggregates, which are not irradiated; light control (LC) containing irradiated aggregates, which are not incubated with TB and untreated, aggregated control (C). The samples were irradiated for different time intervals ranging from 30 to 300 minutes.

Light-induced Inhibition of Tau Aggregates Analyzed by SDS-PAGE

The inhibitory effect of TB on Tau aggregation was observed by SDS-PAGE. Various TB treated reaction mixtures were analyzed at different time intervals. Aggregates have characteristic pattern of higher molecular weight around 250 kDa on SDS-PAGE thus, the effect of TB on aggregation propensity of Tau can be easily observed by SDS-PAGE. Additionally, the gel was subjected to densitometry analysis for quantifying the extent of inhibition occurred in presence of TB. The experiments were done using GE miniVE electrophoresis unit and BIORAD Mini-PROTEAN electrophoresis unit. The gels were scanned in Gel Doc™ XR+ system and the densitometry analysis were done with help of Image Lab™ software.

Transmission Electron Microscopy

For electron microscopic analysis, 2 µM of Tau was incubated on carbon coated copper grids. Following this the samples were negatively stained with 2% uranyl acetate. The images were captured by TECNAI electron microscope at 120 kV.

Dinitrophenylhydrazine (DNPH) Assay

The production of reactive oxygen species (ROS) during PDT was estimated by DNPH assay as described previously by Mesquita *et al.*[25, 26]. Briefly after PDT treatment, the protein was precipitated using 20% trichloroacetic acid (TCA) and pelleted down at 14,000 rpm for 5 minutes. The pellet was re-suspended in 10 mM DNPH dissolved in 2.5 N HCl. After incubating for 60 minutes the protein was pelleted and was washed thrice with ethyl acetate:alcohol (1:1) solution. Finally, the protein was pelleted down at 14,000 rpm for 10 minutes and dissolved in 6 M guanidine hydrochloride. The resultant was analyzed by measuring absorbance at 370 nm. Experiments were carried out in duplicates on soluble full-length Tau.

ROS Production in Neuro2a Cells

The effect of photo-excited TB on ROS production was estimated in N2a cells using DCFDA (2',7'–dichlorofluoresceindiacetate) assay[27, 28]. ROS oxidizes 2,7dichlorofluorescindiacetate to 2', 7' – dichlorofluorescein (DCF) leading to generation of fluorescence. For the assay 10,000 cells/well were seeded in 96 well plate and incubated for 24 hours. The cells were treated with various concentrations of TB following 10 minutes of irradiation in dark. After treatment, the cells were washed subsequently twice with 1X PBS (pH 7.4). The cells were supplemented with 10 µM DCFDA and incubated for 20 minutes. After incubation, the cells were again washed twice with 1X PBS. Finally 100 µL of phenol red free DMEM media was added in each well and fluorescence was measured at 535 nm upon exciting at 485 nm.

Cytotoxicity Assay

The cell viability was analyzed by methylthiazolyldiphenyl-tetrazolium bromide (MTT) assay [29, 30]. N2a cells were cultured in advanced DMEM/F-12 media supplemented with 10% FBS and glutamine. The cells were trypsinized with 0.25% trypsin-EDTA solution. 10,000 cells/well were seeded in 96 well plate for the assays. After 24 hours, the cells were treated with various concentration of TB; followed by addition of MTT at a concentration of 0.5 mg/mL and incubation at 37°C for 4 hours. The formazan crystals formed were dissolved in 100 µL of 100% DMSO. Cell viability was evaluated by measuring the absorbance at 570 nm. Similarly, cells were incubated with 2.5 µM aggregates to observe the cytotoxicity of Tau aggregates; additionally TB was also added to cells along with aggregates for analyzing the effect of TB in presence of aggregates. TB treated cells were subjected to 10 minutes of irradiation for the cytotoxicity analysis of photo-excited TB.

Immunofluorescence

N2a cells were seeded at a density of 50,000 cells on glass cover slips. The cells were treated with various concentration of TB (0.5, 5 and 50 µM) and incubated overnight at 37°C. Similarly, another set of cells treated with various concentration of TB were irradiated with red light for 10 minutes and incubated at 37°C. The cells were fixed with absolute methanol for 20 minutes at -20°C. After fixation cells were permeabilized by 0.2% Triton X-100. After 3 subsequent washes of PBS, the cells were incubated with 5% horse serum for one hour. The cells were incubated with anti-tubulin (Thermo PA1-41331) and K9JA (Dako A0024) antibody. After overnight incubation the cells were incubated with Alexa Fluor 488 (A11034) and Alexa Fluor 555 (A32727) tagged secondary antibodies. The nucleus was stain with DAPI. The samples were scanned by Zeiss Axio observer 7.0, apotome 2.0 inverted microscope using 63X magnifications in oil emersion and at 40% light intensity.

Fly Stocks and Genetics

The transgenic *Drosophila* strain used in this study was UAS-Tau E14. ELAV-Gal4 driver line was obtained from the National Drosophila Stock Center at University of Mysore, Mysore, Karnataka, India. *Drosophila* strains were raised on standard medium. Fly cultures and crosses were carried out at 25°C.

Fly husbandry

Flies were maintained on standard banana-jaggery medium (SM) under standard laboratory conditions of 24±1°C temperature, 75±5% relative humidity, and 12:12 light and dark cycle (SLC)[31]. Flies were maintained in a 2 week discrete generation cycle for 10 generations before being used in this study. The adult density was regulated at about 100 flies per half-pint bottle with 25 mL of SM in 10 bottles. Flies from 10 bottles were combined into a single breeding cage, hereafter referred to as parental cage (PC).

Preparation of TB-supplemented Diet

A total of 2.5 L of SM was prepared following the procedure of and split into 5 batches of 500 mL each[31]. For the control group, SM was poured into the bottles. For the TB-supplemented media, 2.5, 5.0, 10 and 25 μM of TB was added, and mixed thoroughly just before pouring into the bottles. All bottles were plugged with non-adsorbent cotton and the media was allowed to set under room temperature.

Larval Feeding Behavior Assay

The eggs obtained were transferred at a density of 50-eggs/6 mL of SM and allowed to develop till early third instar. The early third instar larvae were removed from the SM vials and used in the feeding behavior assay. Larvae were individually transferred to an assay petri plate of 5 cm diameter containing 10 mL of either liquid SM (SM without agar) or liquid SM supplemented with different concentrations of TB and allowed for 5 seconds for acclimation. The feeding rate was measured as the mean number of sclerite retractions in 2 consecutive 30-second intervals. The average of the 2 rates were taken as the feeding rate of that larva. 20 larvae were assayed for each of the 2 treatment groups. The feeding rate assays were replicated 4 times. A total of 160 larvae were assayed for feeding rate.

Fecundity Assay

Flies from the holding vials were sexed under low CO_2 anesthesia and single pair (one male + one female) was transferred to vial with ~3 mL SM. 20 such vials were set up per treatment, per population. Flies were transferred without anesthesia to fresh SM vials every 24 hours, and the eggs laid during the previous 24 hours were counted under microscope and recorded. The daily egg counts were carried out till the death of female fly in each test vial**.**

Negative Geotaxis Assay

The ability to move against gravity and climb was indicated the level of physical fitness of test animals. Vertical climbing ability of male flies that emerged from different treatment bottles were assessed. Twenty male flies per treatment group were collected and transferred to the empty, 0-15 cm graduated vial. The vial was gently tapped and placed in vertical position. The number of flies that crossed the 15 cm mark in 30 seconds were counted. Three trials were conducted on each set of 20 flies. The data was expressed as percentage of flies that crossed 15 cm mark.

Viability of Fly from Egg to Adult

The eggs from media plate were collected and dispensed into different treatment group of bottles at a density of ~100 eggs/bottle with 45 mL media. Ten bottles each for five treatment groups of SM, SM+ 2, 5, 10 and 25 µM TB were prepared. Bottles were maintained at standard laboratory condition. The flies emerge from different treatments; SM and SM+2, 5, 10 and 25 µM of TB were designated collected and counted. All the assays were carried out on SM using mated flies. The total number of flies that emerged from each bottle were used to calculate the viability of flies emerging from each treatment group.

Larval Olfactory Behavior

The olfactory test was carried out by employing previous method with minor modifications [32]. 30 larvae were briefly dried on a filter paper before being placed in the center of petri dish. The petri dish containing 20 µL of Quinine sulphate dispensed on each of the two 0.5 cm radius filter discs were placed in diametrically opposite position to Quinine zones. After 2 minutes of placing the larvae and covering petri dish, numbers of larvae in different zones were counted to calculate percentage of larvae avoiding the bad odour after training.

Statistical Analysis

Using either duplicate or triplicate reading plotted the statistical data. Untransformed (raw) data were analyzed and plotted by SigmaPlot 10.0 software. The data was analyzed for significance by Student's t-test, where *$p<0.05$, **$p<0.001$, ***$p<0.0001$.

RESULTS

Toluidine Blue interact with Tau in vitro

Tau is a natively unfolded protein, found to be localized majorly in axons and functions to stabilize microtubules. Tau has net basic charge with pI of 8.8, thus for inducing *in-vitro* aggregation of Tau polyanionic co-factors like heparin, arachidonic acid, RNA *etc.,* are being widely applied. Tau protein domain organization comprises of a projection domain and a microtubule-binding domain. The four repeat region of Tau is considered to be the aggregation prone region. The schematic hypothesis depicts the domain organization of full-length Tau and its interaction with TB (Fig. 1A). Toluidine blue is a thiazine dye, which have a characteristic absorption at wavelength 630±10 nm (Fig. 1B). For studying the binding of TB with Tau, changes in UV spectrum of TB with respect to various concentration of Tau were monitored. The UV-visible spectrum indicated a hyperchromic shift in the TB spectra after incubation with various concentration of Tau, which was an indication of interaction between TB and Tau (Fig. 1C). The binding constant (K_D) for TB and Tau was calculated by measuring the long-range spectrum of TB on incubating with various concentrations of full-length Tau. As Tau and TB both had a basic charge, low affinity of TB was observed for Tau. A high K_D value of 14 µM was suggesting the weak interaction between dye and protein., which indicates the interaction (Fig. 1D).

Toluidine Blue inhibits Tau aggregation *in-vitro*

The potency of TB for inhibiting *in-vitro* Tau aggregation was studied. The heparin treated Tau was incubated with various concentrations of TB ranging from 0 to 40 µM. The aggregation was measured by observing ThS fluorescence at different time intervals (Fig. 2A). The result of fluorescence assay suggested that TB potentially inhibited ≥89.2% of Tau aggregation (Fig. 2B). Moreover the morphological changes in TB treated Tau was studied by electron microscopy. The electron micrograph suggested long extended filamentous Tau aggregates in control sample, whereas

TB treated sample has small broken pieces of Tau, which indicated the inefficacy of Tau to aggregate (Fig. 2C, D). The conformation of Tau plays an important role in pathophysiology of AD. In physiological conditions Tau has typical random coil conformation but during aggregation Tau attains β-sheet conformation that absorbs at 220 nm. In our work the changes in secondary structure of Tau aggregates after TB treatment was also studied. The untreated Tau aggregates showed CD spectrum of characteristics peak near β-sheet structure, whereas the TB treated protein found to be at towards random-coil region (Fig. 2E).

Photo-excited Toluidine Blue Disaggregates Tau filaments

The potency of photo-excited TB (PE-TB) in dissolving the pre-formed Tau aggregates was studied by incubating mature Tau fibrils with varying concentrations of PE-TB. In present experiments, TB was irradiated with Red light (630 ±10 nm), which leads to photo-excitation of TB. In our experiments, three controls were taken *viz*. light control, dark control and untreated control. The light control (LC) was consisting of samples, which were irradiated with red light in absence of TB. The aim of light control was to observe the effect of light alone on matured Tau filaments. The dark control (DC) was consist of the protein which were incubated with non-photo excited TB. The motivation for studying dark control was to observe the effect of TB on mature Tau aggregates. Whereas, the untreated control was containing full-length Tau aggregates without any treatment. The effect of PE-TB on Tau disaggregation was characterized by different biochemical and biophysical methods. The SDS-PAGE showed characteristic signature of higher order aggregates in control samples viz. LC, DC and C (Fig. 2F). While the treated samples showed no higher order aggregates on SDS-PAGE. These results firmly indicate the effective role of photo-exited TB in destabilizing preformed Tau aggregates *in vitro*. Moreover, TEM studies revealed the morphological changes in Tau aggregates after PE-TB treatment as after treatment of PE-TB Tau aggregates were disassembled into short and fragile aggregates which was an indication of disaggregation potency of PE-TB for Tau (Fig. 2G, H).

Time-dependent studies of photo-exited Toluidine Blue

The role of irradiation time on potency of PE-TB was analyzed by exposing the aggregates to full-length aggregates for varying time intervals of irradiation of TB. It was observed that irrespective of irradiation time TB had similar effect on disaggregation of Tau. SDS-PAGE analysis indicated the dissolution of aggregates after PDT (Fig. 2I). Further, TEM analysis also revealed the similar characteristics of Tau (Fig. 2J, K). Thus from above data it was apparent that time of irradiation has no significant role on potency of TB.

Quantification of ROS production by photo-excited TB

TB is a photosensitizer thus to study the efficiency of TB to produce singlet oxygen species in cells was estimated by fluorometric DCFDA assay. In our work neuronal cells were treated with various concentrations of TB (Fig. 3A) and photo-excited TB (Fig. 3B) ranging from 0.025 to 2.5 μM. The results indicated that neuroprotective property of TB, as TB generated the low ROS levels. PE-TB deals with the production of singlet oxygen species, which was further quantified and validated by DNPH assay, the protein carbonyl formation of TB treated Tau was targeted to estimate level of ROS (Fig. 3C, D). Under oxidative stress, protein oxidizes to protein carbonyl. DNPH binds to the carbonyl product of protein, forming Schiff's base, which can be quantified at 370 nm. Hence, to determine the ROS production, protein carbonyl quantification has been implied. The increased protein carbonylation after PDT treatment was an indicative of ROS production by TB. The results obtained after treatment of soluble and aggregated Tau protein clearly suggested minimal ROS production by TB, since no significant carbonylation was observed in control and treated protein.

Though being a photosensitizer, TB generates minimal singlet oxygen, which gives it an edge for being potent against Tau and producing low levels of ROS mediated side effects.

Cytotoxicity studies of aggregated Tau and photo-excited Tau

The effect of TB and PE_TB was studied for cellular toxicity. The results suggested that TB was not cytotoxic at 500 nM but increasing the TB dose of 1000 nM a distinct cytotoxicity was observed. (Fig. 4A). Furthermore, in presence of TB the viability of cells was rescued in Tau stressed group (Fig. 4B). TB treated cells were exposed to 10 minutes of irradiation so as to observe the cytotoxicity of PE-TB. The results suggested that up to 500 nM PETB was not toxic to cells, but the high concentration of TB was found to be toxic (Fig. 4C). The results suggested that viability of Tau assaulted N2a cells were rescued in presence of PETB. Morphologically no distinguished change was observed after TB treatment, but the PE-TB treatment lead to the formation of neuronal outgrowths in N2a cells which was indicative of cytoskeleton modulation (Fig. 4D, E). The above observation evidenced the fact that photo-excited TB may modulate the cytoskeleton network of cells.

Toluidine blue modulates the cytoskeleton in neurons

Microtubules are the key component of cytoskeleton network, which assist in maintaining cell integrity, proliferation and division. Microtubules are hollow rod like structures composed of globular protein dimers known as tubulin. In our previous assay we encountered that neuronal cells were efficiently taking up TB as observed by phase contrast microscopy. For further validation of this hypothesis, we studied the effect TB by immunofluorescence assays. In these experiments the cells were tagged with tubulin and Tau specific antibodies. The goal of the study was to check the effect of TB on cytoskeleton. As we found that internalization of TB lead to generation of neurite outgrowth in cells. Similar to earlier results the cells tagged with anti-tubulin antibody showed no change in cell morphology and tubulin .The cells treated with lower concentration of TB (0.5 µM) found to have healthy morphology with long neurite outgrowth and high tubulin expression. On contrary a higher concentration of 5 µM TB and photo-excited TB generates toxicity to the cells leading to change in cell morphology. Additionally, the cells were also tagged with pan-Tau K9JA antibody to observe the intrinsic levels of Tau expression. The treatment showed increased intrinsic Tau expression, which supports the fact that photo-excited TB, is modulating the cytoskeleton network. The fluorescence images of single neuronal cells clearly indicated that distribution of Tubulin and Tau was increased after PDT treatment. The distribution of Tau and tubulin in neuron was clearly observed in the florescent microscopic images of single neuronal cells (Fig. 5A, B). Morphological changes of cells were observed by differential interference contrast (DIC) images. The DIC images suggest that at 0.5 µM TB cells were having a conventional cellular morphologically similar to control which have intact nucleus, long extensions and enlarged cell soma, whereas, as concentration of TB increased to 5 µM and above TB cells showed reduced extension and shrunken soma, which was indicative to cytotoxicity.

The effect of TB and photo-excited TB on Tau transgenic *Drosophila* model

The over expression of Tau in nervous system of *Drosophila* mimics Tauopathy, the neuronal accumulation of Tau aggregates leading to abnormal behavior in *Drosophila*. The effect of TB and photo-excited TB on various behavioral aspects of UAS-E14 Tau mutant *Drosophila* was studied. *Drosophila* behavioral studies were carried out in two sets; the first set with TB and the other was with photo-excited dye. The parameters chosen for the studies were feeding behavior, locomotory dysfunction, loss of memory and potency to reproduce. The current data suggest that photo-excited TB has a rescuing effect on transgenic flies (Fig. 6A). The flies treated with photo-excited TB

showed increased food uptake when compared to the group exposed to TB. There was no concentration dependent change in either sets of TB exposure (Fig. 6B). The next set of experiments was carried out to analyze the effect of TB and photo-excited TB on olfactory sensation of *Drosophila* larvae, basically the ability to avoid bad odor. The objective behind the experiment was to check the memory deficit in UAS Tau E14 transgenic *Drosophila* larvae after treatment with dye. The transgenic UAS Tau E14 larvae were unable to avoid the odor efficiently as compared to wild type flies. TB treatment restored olfactory sensation indicating potency of TB to affect nervous system of E14 Tau *Drosophila*. Here, the photo-excited dye showed more potency over non photo-excited TB. In case of concentration-dependent treatment a bell shaped pattern was observed which indicate that 5 μM of photo-excited TB has maximum activity in restoring olfactory sensation of flies (Fig. 6C). Succeeding experiments were performed to examine the effect of TB and photo-excited TB on locomotor system in Tau flies. Negative geotaxis assay was performed and the numbers of flies escaped were plotted against time to interpret results in terms of percentage. The results showed similar bell shaped pattern as earlier experiment. The 5 μM of photo-excited TB was estimated to be potent concentration for rehabilitating the locomotors activity of flies (Fig. 6D). Furthermore, the effect of TB and photo-excited TB was observed on the longevity of flies. For this objective two assay *viz.* viability assay and fecundity assay were carried out. It was observed that photo-excited TB increases the longevity of flies more efficiently than TB. After the treatment of dye, survival and egg laying ability of flies were increased and a bell shaped pattern was observed indicating the efficiency of 5 μM dye to increase survival of Tauopathy *Drosophila* mutant UAS Tau E14 flies (Fig. 7A, B). The overall experimental data concluded that TB was effective in restoring the adverse effect of Tauopathy in Tau E14 flies. Additionally photo-excited TB was more effective than non-photo-excited TB. Out of all spectrums of concentrations, 5 μM of TB and photo-excited TB was found to be optimal and most effective concentration in treating *Drosophila* Tauopathy.

DISCUSSION

Pathological Tau leads to generation of PHFs, which are characteristic features of AD[8]. The importance of small molecules have been reported, which includes the synthetic and naturally originated compounds[33, 34]. Dyes were tested thoroughly for their medicinal property because of being inexpensive, highly specific and more potent. Their photo-excitation property was explored against various protein aggregates including Amyloid-β, Tau and Prion *etc.*[16, 35]. Toluidine blue is a phenothiazine dye; reported, which has known to decrease the AD pathology. TB was reported to decrease the secretion of pathological Amyloid β 40 and Amyloid-β 42[36]. Furthermore TB found to modulate the amyloid protein mediated pathology in hippocampus, on contrary TB was unable to rescue the Tau phosphorylation in transgenic 3xTg mice [36]. Moreover, TB not only reported to be a amyloid proteins modulator, it also reported to restore the cholinergic hormone secretion in brain thus recuing the neural degeneration [37]. In present study we investigated the effects of TB and photo-excited TB against Tau aggregation. MB, the parent compound of TB has been reported in literature as a potent Tau aggregation inhibitor. In our experiments K_D value of 14 μM with a hyperchromic shift in spectrum indicated low binding affinity of TB for full-length Tau, which could be due to the basic charge of TB. The data obtained suggest a hypochromic shift at 630 nm in TB spectra in presence of Tau. However, in this contemporary study, the potency of photo-excited TB in dissolving the preformed Tau aggregates have also been analyzed by various biochemical and biophysical methods such as SDS-PAGE, CD spectroscopy, ThS fluorescence and electron microscopy Additionally, TB possesses the tendency of photo-excitation like its parent compound

MB and exposure at 630 nm leads to generation of singlet oxygen species[38]. The ThS binding revealed the effect of TB in inhibiting the aggregation of Tau. The aggregates formed were analyzed qualitatively using TEM, which details the effect of small molecules on aggregates morphology. The phenothiazine dye MB methylene blue effectively inhibited Tau aggregates formation[39]. But other dyes such as methyl yellow, azo dye and ponceau, a sulfonated dye had no effect on Tau aggregation [11] The morphology of Tau in presence of TB evidenced the potential in prevent in aggregates formation, which resulted in fragmented filaments. The protein loses its native conformation during aggregation and this was signified by change in absorbance in far-UV region. Studies showed that photo-excited MB prevented the conformational changes in Amyloid-β from random coil to β-sheet rich structure[10]. Similarly, TB also prevented conformational changes in Tau and maintained its random coil conformation.

Irradiation of photosensitizer will lead to the generation of its photoactive form. In relevance to the previous studies, time of irradiation did not play significant role, which indicate that only a short period of irradiation led to threshold energy for photo-excitation of TB[40]. The quantitative results obtained after PDT treatment were supported by electron microscopy which showed the broken filaments in treated samples instead of long inter-tangled filamentous structure of Tau aggregates[41]. Generation of singlet oxygen species is the characteristic of a photosensitizer, being a potent photosensitizer the TB generates singlet oxygen [42, 43]. ROS production has detrimental effects on cells hence, the effect of TB and photo-excited TB on ROS production was estimated by fluorometry[44]. The minimal generation of ROS by photo-excited TB project it's a biocompatible photo-sensitizer, which can be further implied in vivo to check its efficiency. Furthermore, since aggregates lead to generation of ROS, we investigated the effect of TB ROS generated by Tau aggregates[45-47]. Our findings suggested that TB have moderate cytotoxic potency at lower concentrations [48]. Additionally they protect cells from oxidative stress and other toxic insults[49]. Similar results were observed in present experiments, which evidenced TB to be non-toxic in N2a cells up to 2.5 μM. There are studies suggesting the fact that treatment of natural compounds such as curcumin and resveratrol increases the neurite outgrowths and help in normal proliferation of cells[50]. Similarly *via.* high throughput screening compounds like ceravastatin has been identified as a neurite growth accelerator[51]. Likewise in our experiments TB and photo-excited TB found to increase the neurite outgrowth and tubulin expression in N2a cells. Drosophila has been proven to be an ideal model for neurodegenerative diseases. Several mutants of drosophila have been reported in context to Tauopathy [52]. Recently the studies stated that photo-excited MB decreased the vacuole formation in *Drosophila* brain indicating the rescue from neurodegeneration [53]. Human Tau pathology has been effectively modeled in *Drosophila, which* was based on overexpression of mutant Tau in fly brain. The photo-excited TB rescued the Tauopathy in *Drosophila*. We found that photo-excited TB reversed Tauopathy induced neurodegenerative phenotypic disorders like olfactory disability, reproductive potentiality and loss of memory and locomotory disability in UAS Tau E14 *Drosophila* mutants. The behavioral deficits were targeted for studying effect of Tau expression in *Drosophila* neuron. These results indicate that photo-excited TB could suppress behavioral defects by reducing the formation of Tau aggregates in *Drosophila* brain. Collectively, behavioral analysis in *Drosophila* indicates that Tauopathy-induced behavioral defects were rescued after TB treatment. Neurons are essential for olfactory learning, which is elicited by memory retrieval or stability. This underlies the cognitive deficits observed early in many Tauopathies. The overall studies on TB in various *in-vitro* and *in-vivo* systems strongly support its efficiency against AD-related Tauopathy (Fig. 8).

Acknowledgements
This project is supported in part by grants from the in-house, National Chemical Laboratory-Council of Scientific Industrial Research-(CSIR-NCL) grant MLP029526. Tau constructs were kindly gifted by Prof. Roland Brandt from University of Osnabruck, Germany. Tushar Dubey and Nalini Vijay Gorantla acknowledges the fellowship from University of Grant Commission (UGC), India.

Competing Financial Interests
The authors declare no competing financial interest.

Additional information
Supplementary information accompanies this paper at https://pubs.acs.org

Author Information
Tushar Dubey, Nalini Vijay Gorantla and Subashchandrabose Chinnathambi
Neurobiology Group, Division of Biochemical Sciences, CSIR-National Chemical Laboratory, Dr. Homi Bhabha Road, 411008 Pune, India
Tushar Dubey, Nalini Vijay Gorantla and Subashchandrabose Chinnathambi
Academy of Scientific and Innovative Research (AcSIR), 110025 New Delhi, India
Kagepura Thammaiah Chandrashekara
Institution of Excellence, Vijnana Bhavan, University of Mysore, Manasagangotri, Mysore, 570006

Author Contributions
T.D, N.V and S.C designed the experiments. T.D and N.V carried out the experiments. T.D, N.V and S.C analyzed the data. T.D, N.V and S.C wrote the article. *Drosophila* studies were carried out by K.T.C. S.C. conceived the idea of the project. All authors contributed to the discussions and manuscript review.

Corresponding Author
Correspondence and requests for materials should be addressed to **Prof. Subashchandrabose Chinnathambi. Email:** s.chinnathambi@ncl.res.in
Telephone: +91-20-25902232, Fax. +91-20-25902648.

ORCID
Subashchandrabose Chinnathambi: 0000-0002-5468-2129

Additional information
Supplementary information accompanies this paper at https://www.acs.com/articles.

Abbreviations
AD, Alzheimer's disease; PHFs, Paired Helical Filaments; NFTs, Neurofibrillary Tangles; TB, Toluidine Blue; MB, Methylene Blue; PDT, Photodynamic Therapy; ThS, Thioflavin S; MTT, Methylthiazolyldiphenyl-tetrazolium bromide; SEC, Size Exclusion Chromatography; BCA, Bicinchoninic acid; DMSO, Dimethyl sulfoxide; DNPH, Dinitrophenylhydrazine; ROS, Reactive oxygen species; SDS-PAGE, Sodium dodecyl sulfate-polyacrylamide gel electrophoresis; TEM, Transmission electron microscopy; BSA, Bovine serum albumin.

Figures legends

Figure 1. Tau interacts with Toluidine Blue. A) Schematic hypothesis of Tau aggregation inhibition by TB. The bar diagram demonstrate the domain organization of 441 amino acid long full-length Tau. Structurally Tau can be divided in two domains *viz.,* projection domain and microtubule-binding domain. The four repeat regions contribute majorly in aggregation of Tau and the proline rich region is target for many post-translation modifications. B) UV-visible absorption spectra of TB showing the absorption maxima at 630 nm. C) The absorption spectrum of TB in presence of various concentrations of full-length human Tau in the visible region at around 314 nm. In presence of Tau, hyperchromic shift was observed in TB spectrum, which indicates binding of Tau to TB. D) The absorbance maxima curve of TB in presence of full-length Tau at fixed wavelength of 630 nm. The hyperbolic curve was observed with K_D value of 14 μM.

Figure 2. Tau inhibition by Toluidine Blue. A) The effect of TB to inhibit Tau aggregation was monitored by ThS fluorescence assay. B) Quantification of the rate of aggregation inhibition by TB. C) The electron micrograph of Tau aggregates reveals long fibrillar morphology of Tau aggregates whereas; in presence of TB small broken fibrils were observed. D) The qualitative analysis of Tau aggregates by TEM after incubating with TB exhibited the population of small, broken filaments after PDT treatment. This indicates the potency of TB in disintegrating Tau aggregates. E) Native Tau has random coil conformation but as it aggregates it obtains β-sheet conformation. Treatment with TB inhibited the conformational change in Tau, in concentration dependent manner. F) SDS-PAGE analysis of Tau aggregates treated with varying concentration of photo-excited TB ranging from 2 to 40 μM demonstrated clear decrease in higher order aggregates. These results indicate the effective role of PDT against higher order aggregates. The red box indicated the disappearance of higher order aggregates on SDS-PAGE, which apparent in control groups. G) The electron microscopy showed long thick matured fibrils of Tau. H) Qualitative analysis of Tau aggregates by TEM after incubating with photo-excited TB exhibited the population of small, broken filaments. This indicates the potency of TB in disintegrating Tau aggregates. I) SDS-PAGE analysis of TB treated Tau aggregates irradiated for various irradiation times (30 to 300 minutes). The SDS-PAGE clearly suggests the difference between irradiated and non-irradiated Tau aggregates. The red box indicates the disappearance of higher order aggregates on SDS-PAGE, which was apparent in control groups. (J, K) The qualitative analysis of Tau aggregates after 30 and 300 minutes of irradiation. The broken filaments observed under electron microscope were indicative of disaggregation. The significance was calculated using student *t-test* in Sigma Plot 10.0. *$p<0.05$, **$p<0.001$, ***$p<0.0001$, the statistical difference between control and treated groups.

Figure 3. Reactive oxygen species production. A) The DCFDA assay indicates the extent of ROS production by photo-excited TB in N2a cells treated with 2.5 μM full-length Tau aggregates. These data suggests that in presence of TB low levels of ROS were produced. The results indicate that in comparison to aggregated Tau, soluble Tau generates minimal ROS. B) Fluorescence microscopic analysis of N2a cells reveled the changes in morphology of cells upon treatment with Tau aggregates. C) A concentration dependent increase in ROS production was observed after analyzing the carbonylation of full-length Tau aggregates after irradiation. D) Negligible levels of carbonylation in soluble Tau were observed after treatment with photo-excited TB. The significance was calculated using student t-test in SigmaPlot 10.0. *$p<0.05$, **$p<0.001$, ***$p<0.0001$, the statistical difference between control and treated groups.

Figure 4. Cell viability of TB-induced Tau. Cytotoxicity assay of TB and photo-excited TB was performed using MTT assay in N2a cells. Cells were treated with varying concentration of TB ranging from 0.025 to 2.5 μM. A) The effect of TB on cell viability was analyzed by MTT assay. TB had no cytotoxic effect on cells at concentration as high as 0.5 μM. B) MTT analysis showed that presence of TB rescued cell viability after exposing to Tau aggregates. C) Photo-exited TB exhibited protective role on cell viability in Tau stressed cells. D, E) The cell morphology did not alter after exposure to TB and photo-excited TB, which indicates healthy cells.

Figure 5. Modulation of cytoskeleton network by PE-TB A) The cells were treated with various concentrations of TB. At lower concentration TB (0.5 μM) showed high expression of tubulin with increased neurite outgrowth whereas, high TB concentration (5 μM) found to be toxic to cells. The photo-excited TB also showed extended neurite outgrowth at lower concentration whereas, 5 μM photo-excited TB was cytotoxic. B) The fluorescent image of tubulin stained single neuronal cell suggesting that distribution of tubulin was prominently in neurite outgrowths and Tau was distributed all over cell soma.

Figure 6. The effect of TB and PE-TB on locomotary behavior of transgenic drosophila flies. A) The transgenic flies were exposed to TB and photo-excited TB for various time points at different stages of life cycle to study the effect of TB in restoring memory deficit, locomotory dysfunction and viability. B) The results suggest the effect of various concentrations of TB and photo-excited TB on feeding behavior of flies. The photo-excited TB found to be more potent than non-photo-excited TB. C) The E14 Tau flies were exposed to various concentrations of TB to analyze changes in olfactory sensation by avoiding the bad odor of quinine. 5 μM of photo-excited TB demonstrated appreciable potency in restoring the olfaction. D) The negative geotaxis assay was performed to examine the effect of TB on locomotion of flies. The bell shaped graph indicated 5 μM of photo-excited TB to be effective in rescuing locomotory system of E14 tau drosophila. The significance was calculated using student t-test in Sigma Plot 10.0. *$p<0.05$, **$p<0.001$, ***$p<0.0001$, the statistical difference between control and treated groups before photo-excitation. #$p<0.05$, ##$p<0.001$, ###$p<0.0001$, the statistical difference between control and treated groups after photo-excitation

Figure 7. TB and PE-TB increase the longevity of transgenic drosophila flies. Viability assays were carried out to analyze survival rate of E14 Tau transgenic flies from egg to adults after exposure to TB. A) The data indicates 5 μM of TB to have appreciable effect on survival rate of transgenic flies. B) The fecundity assay was carried out to check the fitness of flies. The bell shaped pattern was indicates that 5 μM of photo-excited TB exposure increased egg laying or reproducibility in female E14 Tau drosophila flies. The significance was calculated using student t-test in Sigma Plot 10.0. *$p<0.05$, **$p<0.001$, ***$p<0.0001$, the statistical difference between control and treated groups before photo-excitation. #$p<0.05$, ##$p<0.001$, ###$p<0.0001$, the statistical difference between control and treated groups after photo-excitation.

Figure 8. Schematic diagram of Tau aggregation inhibition by photo-excited TB. Tau under pathological conditions leads to generation of paired helical filaments. TB and its photo-excited form have potential to inhibit the Tau aggregation as well as it disaggregates mature Tau fibril respectively. This dual property of TB makes it an influential therapeutic molecule in the field of AD. TB treatment rescued the memory deficit and viability in Tauopathy model of *Drosophila.*

References

1. Arriagada, P. V., Growdon, J. H., Hedley-Whyte, E. T., and Hyman, B. T. (1992) Neurofibrillary tangles but not senile plaques parallel duration and severity of Alzheimer's disease, *Neurology 42*, 631-631.
2. Selkoe, D. J. (1991) The molecular pathology of Alzheimer's disease, *Neuron 6*, 487-498.
3. Forman, M. S., Trojanowski, J. Q., and Lee, V. M. Y. (2004) Neurodegenerative diseases: a decade of discoveries paves the way for therapeutic breakthroughs, *Nature medicine 10*, 1055-1063.
4. Morris, M., Maeda, S., Vossel, K., and Mucke, L. The many faces of tau, *Neuron 70*, 410-426.
5. Giacobini, E., and Gold, G. Alzheimer disease therapyâ€"moving from amyloid-Î² to tau, *Nature Reviews Neurology 9*, 677-686.
6. Mandelkow, E.-M., and Mandelkow, E. Biochemistry and cell biology of tau protein in neurofibrillary degeneration, *Cold Spring Harbor perspectives in medicine 2*, a006247.
7. Obulesu, M., Venu, R., and Somashekhar, R. Tau mediated neurodegeneration: an insight into Alzheimerâ€™s disease pathology, *Neurochemical research 36*, 1329-1335.
8. Wang, Y., and Mandelkow, E. Tau in physiology and pathology, *Nature Reviews Neuroscience 17*, 22-35.
9. Oz, M., Lorke, D. E., and Petroianu, G. A. (2009) Methylene blue and Alzheimer's disease, *Biochemical pharmacology 78*, 927-932.
10. Akoury, E., Pickhardt, M., Gajda, M., Biernat, J., Mandelkow, E., and Zweckstetter, M. Mechanistic basis of phenothiazineâ€ driven inhibition of Tau aggregation, *Angewandte Chemie International Edition 52*, 3511-3515.
11. Taniguchi, S., Suzuki, N., Masuda, M., Hisanaga, S.-i., Iwatsubo, T., Goedert, M., and Hasegawa, M. (2005) Inhibition of heparin-induced tau filament formation by phenothiazines, polyphenols, and porphyrins, *Journal of Biological Chemistry 280*, 7614-7623.
12. Pakavathkumar, P., Sharma, G., Kaushal, V., Foveau, B., and LeBlanc, A. C. (2015) Methylene blue inhibits caspases by oxidation of the catalytic cysteine, *Scientific reports 5*, 13730.
13. Atamna, H., and Kumar, R. (2010) Protective role of methylene blue in Alzheimer's disease via mitochondria and cytochrome c oxidase, *Journal of Alzheimer's Disease 20*, S439-S452.
14. Moloney, A., Sattelle, D. B., Lomas, D. A., and Crowther, D. C. (2010) Alzheimer's disease: insights from Drosophila melanogaster models, *Trends in biochemical sciences 35*, 228-235.
15. Tan, F. H. P., and Azzam, G. (2017) Drosophila melanogaster: Deciphering Alzheimerâ€™s Disease, *The Malaysian journal of medical sciences: MJMS 24*, 6.
16. Janouskova, O., Rakusan, J., Karaskova, M., and Holada, K. Photodynamic inactivation of prions by disulfonated hydroxyaluminium phthalocyanine, *Journal of General Virology 93*, 2512-2517.
17. Lee, B. I., Lee, S., Suh, Y. S., Lee, J. S., Kim, A. k., Kwon, O. Y., Yu, K., and Park, C. B. Photoexcited Porphyrins as a Strong Suppressor of Î²â€Amyloid Aggregation and Synaptic Toxicity, *Angewandte Chemie 127*, 11634-11638.
18. Wischik, C. M., Harrington, C. R., and Storey, J. M. D. Tau-aggregation inhibitor therapy for Alzheimer's disease, *Biochemical pharmacology 88*, 529-539.
19. Bolkan, B. J., and Kretzschmar, D. (2014) Loss of Tau results in defects in photoreceptor development and progressive neuronal degeneration in Drosophila, *Developmental neurobiology 74*, 1210-1225.
20. Gorantla, N. V., Khandelwal, P., Poddar, P., and Chinnathambi, S. Global Conformation of Tau Protein Mapped by Raman Spectroscopy, *Tau Protein: Methods and Protocols*, 21-31.
21. Barghorn, S., Biernat, J., and Mandelkow, E. (2005) Purification of recombinant tau protein and preparation of Alzheimer-paired helical filaments in vitro, *Amyloid Proteins: Methods and Protocols*, 35-51.
22. Barghorn, S., Biernat, J., and Mandelkow, E. (2005) Purification of recombinant tau protein and preparation of Alzheimer-paired helical filaments in vitro. In *Amyloid proteins* pp 35-51, Springer.
23. Santa-MarÃ-a, I., PÃ©rez, M., HernÃ¡ndez, F. l., Avila, J. s., and Moreno, F. J. (2006) Characteristics of the binding of thioflavin S to tau paired helical filaments, *Journal of Alzheimer's Disease 9*, 279-285.
24. Gorantla, N. V., Shkumatov, A. V., and Chinnathambi, S. Conformational Dynamics of Intracellular Tau Protein Revealed by CD and SAXS, *Tau Protein: Methods and Protocols*, 3-20.
25. Mesquita, C. S., Oliveira, R., Bento, F. t., Geraldo, D., Rodrigues, J. o. V., and Marcos, J. o. C. Simplified 2, 4-dinitrophenylhydrazine spectrophotometric assay for quantification of carbonyls in oxidized proteins, *Analytical biochemistry 458*, 69-71.
26. Fagan, J. M., Sleczka, B. G., and Sohar, I. (1999) Quantitation of oxidative damage to tissue proteins, *The international journal of biochemistry & cell biology 31*, 751-757.
27. Alexandre, J. r. m., Batteux, F. d. r., Nicco, C., ChÃ©reau, C., Laurent, A., Guillevin, L. c., Weill, B., and Goldwasser, F. o. (2006) Accumulation of hydrogen peroxide is an early and crucial step for paclitaxelâ€induced cancer cell death both in vitro and in vivo, *International journal of cancer 119*, 41-48.
28. Degli Esposti, M. (2002) Measuring mitochondrial reactive oxygen species, *Methods 26*, 335-340.

29. Pasinelli, P., Borchelt, D. R., Houseweart, M. K., Cleveland, D. W., and Brown, R. H. (1998) Caspase-1 is activated in neural cells and tissue with amyotrophic lateral sclerosis-associated mutations in copper-zinc superoxide dismutase, *Proceedings of the National Academy of Sciences 95*, 15763-15768.
30. Fioriti, L., Dossena, S., Stewart, L. R., Stewart, R. S., Harris, D. A., Forloni, G., and Chiesa, R. (2005) Cytosolic prion protein (PrP) is not toxic in N2a cells and primary neurons expressing pathogenic PrP mutations, *Journal of Biological Chemistry 280*, 11320-11328.
31. Chandrashekara, K. T., and Shakarad, M. N. (2011) Aloe vera or resveratrol supplementation in larval diet delays adult aging in the fruit fly, Drosophila melanogaster, *Journals of Gerontology Series A: Biomedical Sciences and Medical Sciences 66*, 965-971.
32. Heisenberg, M., Borst, A., Wagner, S., and Byers, D. (1985) Drosophila mushroom body mutants are deficient in olfactory learning, *Journal of neurogenetics 2*, 1-30.
33. Calcul, L., Zhang, B., Jinwal, U. K., Dickey, C. A., and Baker, B. J. Natural products as a rich source of tau-targeting drugs for Alzheimerâ€™s disease, *Future medicinal chemistry 4*, 1751-1761.
34. Pickhardt, M., Neumann, T., Schwizer, D., Callaway, K., Vendruscolo, M., Schenk, D., St George-Hyslop, P., M Mandelkow, E., M Dobson, C., and McConlogue, L. Identification of small molecule inhibitors of tau aggregation by targeting monomeric tau as a potential therapeutic approach for tauopathies, *Current Alzheimer Research 12*, 814-828.
35. Lee, B. I., Suh, Y. S., Chung, Y. J., Yu, K., and Park, C. B. Shedding Light on Alzheimerâ€™s Î²-Amyloidosis: Photosensitized Methylene Blue Inhibits Self-Assembly of Î²-Amyloid Peptides and Disintegrates Their Aggregates, *Scientific Reports 7*, 7523.
36. Yuksel, M., Biberoglu, K., Onder, S., Akbulut, K. G., and Tacal, O. (2017) Effects of phenothiazine-structured compounds on APP processing in Alzheimer's disease cellular model, *Biochimie 138*, 82-89.
37. Biberoglu, K., Tek, M. Y., Ghasemi, S. T., and Tacal, O. (2016) Toluidine blue O is a potent inhibitor of human cholinesterases, *Archives of biochemistry and biophysics 604*, 57-62.
38. Page, K., Wilson, M., and Parkin, I. P. (2009) Antimicrobial surfaces and their potential in reducing the role of the inanimate environment in the incidence of hospital-acquired infections, *Journal of Materials Chemistry 19*, 3819-3831.
39. Wischik, C. M., Edwards, P. C., Lai, R. Y., Roth, M., and Harrington, C. R. (1996) Selective inhibition of Alzheimer disease-like tau aggregation by phenothiazines, *Proceedings of the National Academy of Sciences 93*, 11213-11218.
40. Medina, D. X., Caccamo, A., and Oddo, S. Methylene blue reduces AÎ² levels and rescues early cognitive deficit by increasing proteasome activity, *Brain pathology 21*, 140-149.
41. Alonso, A. d. C., Grundke-Iqbal, I., and Iqbal, K. (1996) Alzheimer's disease hyperphosphorylated tau sequesters normal tau into tangles of filaments and disassembles microtubules, *Nature medicine 2*, 783-787.
42. KÃ¶merik, N., Nakanishi, H., MacRobert, A. J., Henderson, B., Speight, P., and Wilson, M. (2003) In vivo killing of Porphyromonas gingivalis by toluidine blue-mediated photosensitization in an animal model, *Antimicrobial agents and chemotherapy 47*, 932-940.
43. Bouillaguet, S., Wataha, J. C., Zapata, O., Campo, M., Lange, N., and Schrenzel, J. Production of reactive oxygen species from photosensitizers activated with visible light sources available in dental offices, *Photomedicine and laser surgery 28*, 519-525.
44. Eruslanov, E., and Kusmartsev, S. Identification of ROS using oxidized DCFDA and flow-cytometry, *Advanced protocols in oxidative stress II*, 57-72.
45. Zhang, W., Wang, T., Pei, Z., Miller, D. S., Wu, X., Block, M. L., Wilson, B., Zhang, W., Zhou, Y., and Hong, J.-S. (2005) Aggregated Î±-synuclein activates microglia: a process leading to disease progression in Parkinsonâ€™s disease, *The FASEB Journal 19*, 533-542.
46. Schilling, T., and Eder, C. Amyloidâ€Î²â€induced reactive oxygen species production and priming are differentially regulated by ion channels in microglia, *Journal of cellular physiology 226*, 3295-3302.
47. Zraika, S., Hull, R. L., Udayasankar, J., Aston-Mourney, K., Subramanian, S. L., Kisilevsky, R., Szarek, W. A., and Kahn, S. E. (2009) Oxidative stress is induced by islet amyloid formation and time-dependently mediates amyloid-induced beta cell apoptosis, *Diabetologia 52*, 626-635.
48. Tremblay, J.-F. o., Dussault, S., Viau, G., Gad, F., Boushira, M. l., and Bissonnette, R. (2002) Photodynamic therapy with toluidine blue in Jurkat cells: cytotoxicity, subcellular localization and apoptosis induction, *Photochemical & Photobiological Sciences 1*, 852-856.
49. Harrington, C. R., Storey, J. M. D., Clunas, S., Harrington, K. A., Horsley, D., Ishaq, A., Kemp, S. J., Larch, C. P., Marshall, C., and Nicoll, S. L. Cellular models of aggregation-dependent template-directed proteolysis to characterize tau aggregation inhibitors for treatment of Alzheimer disease, *Journal of Biological Chemistry 290*, 10862-10875.
50. Bora-Tatar, G., and Erdem-Yurter, H. Investigations of curcumin and resveratrol on neurite outgrowth: perspectives on spinal muscular atrophy, *BioMed research international 2014*.

51. Sherman, S. P., and Bang, A. G. High-throughput screen for compounds that modulate neurite growth of human induced pluripotent stem cell derived neurons, *Disease models & mechanisms*, dmm. 031906.
52. Iijima-Ando, K., and Iijima, K. (2010) Transgenic Drosophila models of Alzheimer's disease and tauopathies, *Brain Structure and Function 214*, 245-262.
53. Lee, B. I., Suh, Y. S., Chung, Y. J., Yu, K., and Park, C. B. (2017) Shedding Light on Alzheimer's β-Amyloidosis: Photosensitized Methylene Blue Inhibits Self-Assembly of β-Amyloid Peptides and Disintegrates Their Aggregates, *Scientific reports 7*, 7523.

Figures

Figure 1

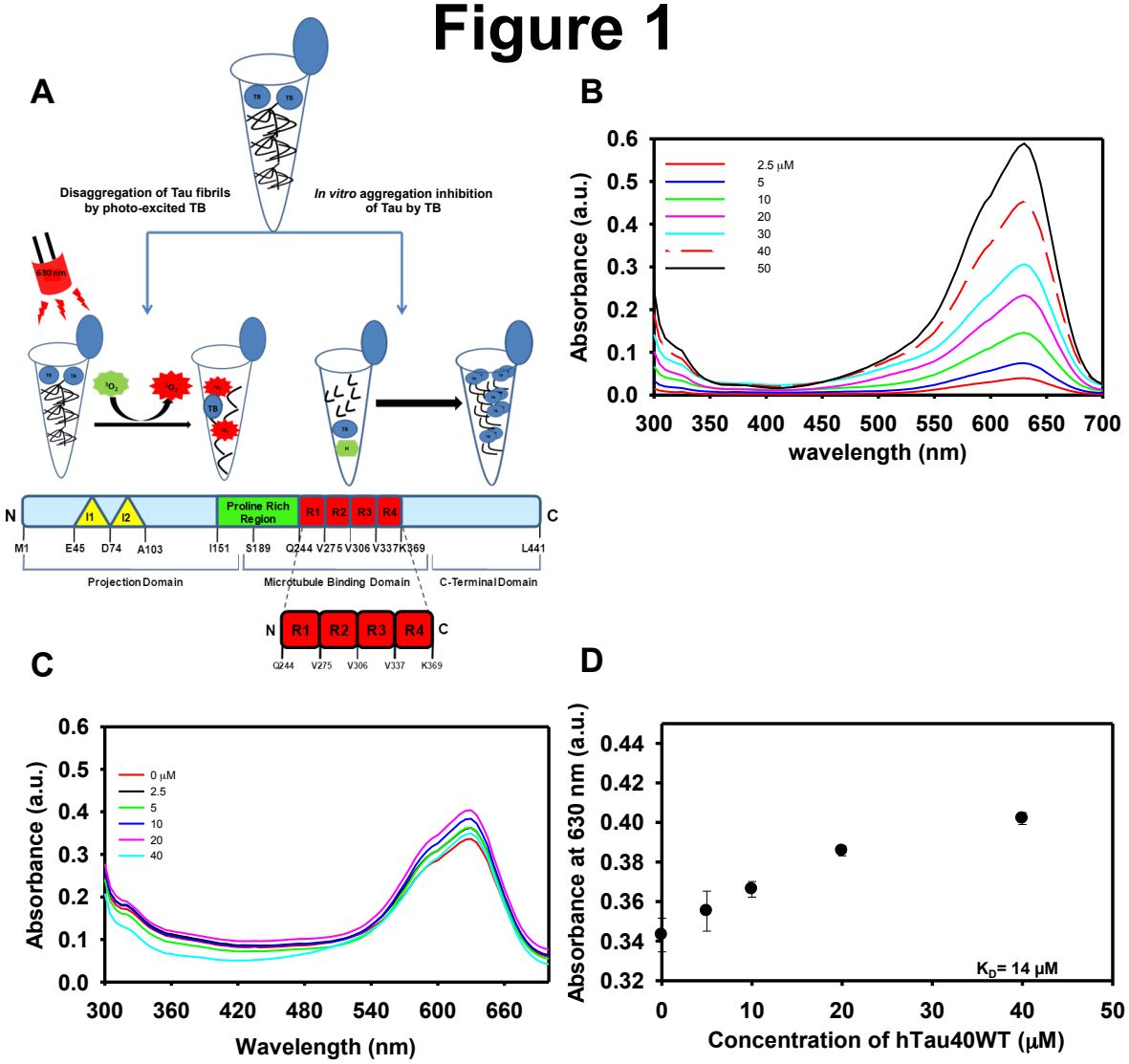

Figure 2

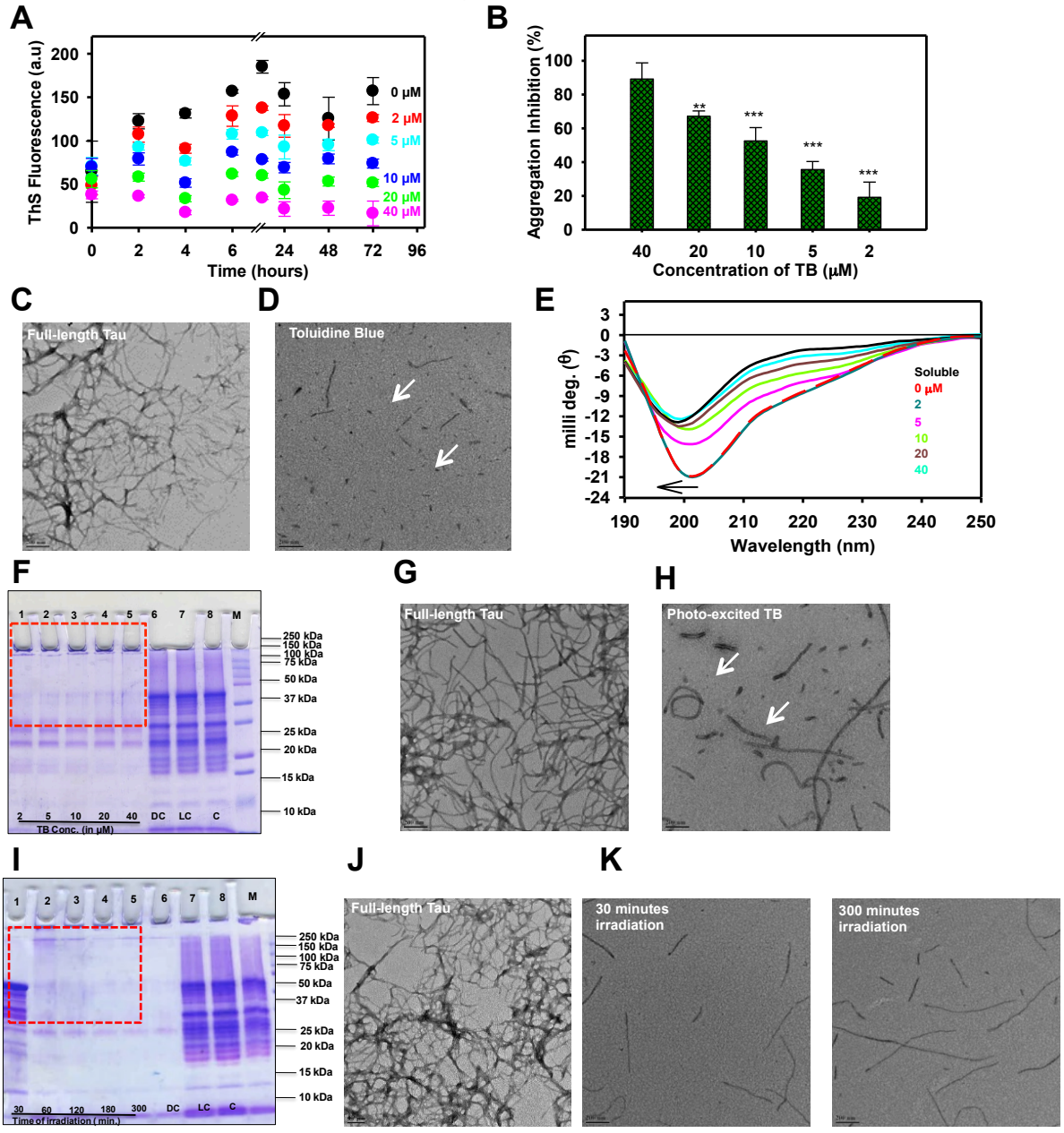
A
ThS Fluorescence (a.u)
Time (hours)
0 µM
2 µM
5 µM
10 µM
20 µM
40 µM
B
Aggregation Inhibition (%)
Concentration of TB (µM)
C
Full-length Tau
D
Toluidine Blue
E
milli deg. (θ)
Wavelength (nm)
Soluble
0 µM
2
5
10
20
40
F
250 kDa
150 kDa
100 kDa
75 kDa
50 kDa
37 kDa
25 kDa
20 kDa
15 kDa
10 kDa
TB Conc. (in µM)
DC
LC
C
G
Full-length Tau
H
Photo-excited TB
I
Time of irradiation (min.)
J
Full-length Tau
K
30 minutes irradiation
300 minutes irradiation

Figure 3

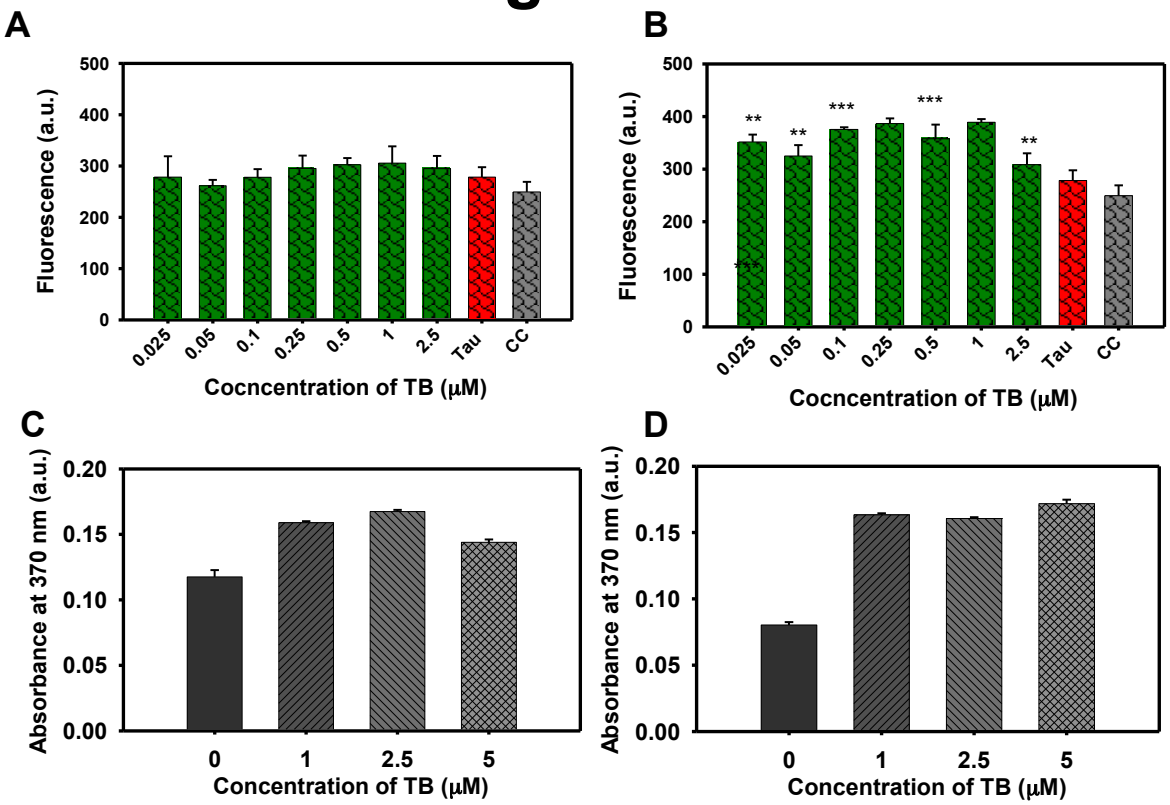
A
B
C
D
Fluorescence (a.u.)
Cocncentration of TB (μM)
Absorbance at 370 nm (a.u.)
Concentration of TB (μM)
0.025
0.05
0.1
0.25
0.5
1
2.5
Tau
CC
0
1
2.5
5

Figure 4

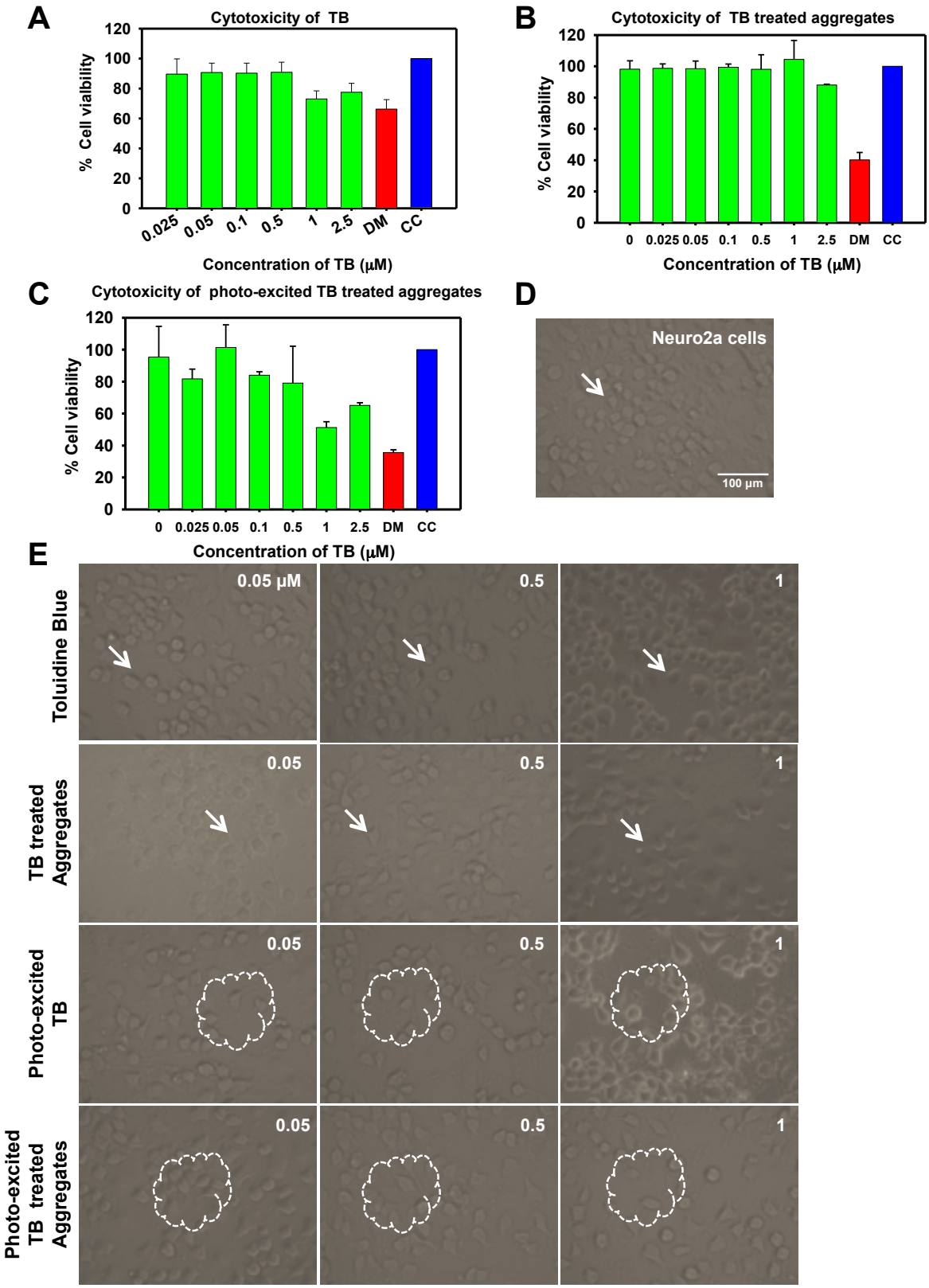
A
Cytotoxicity of TB
% Cell vialbility
120
100
80
60
40
20
0
0.025
0.05
0.1
0.5
1
2.5
DM
CC
Concentration of TB (μM)
B
Cytotoxicity of TB treated aggregates
% Cell viability
0
0.025
0.05
0.1
0.5
1
2.5
DM
CC
Concentration of TB (μM)
C
Cytotoxicity of photo-excited TB treated aggregates
% Cell viability
Concentration of TB (μM)
D
Neuro2a cells
100 μm
E
Toluidine Blue
TB treated Aggregates
Photo-excited TB
Photo-excited TB treated Aggregates
0.05 μM
0.5
1
0.05
0.5
1
0.05
0.5
1
0.05
0.5
1

Figure 5

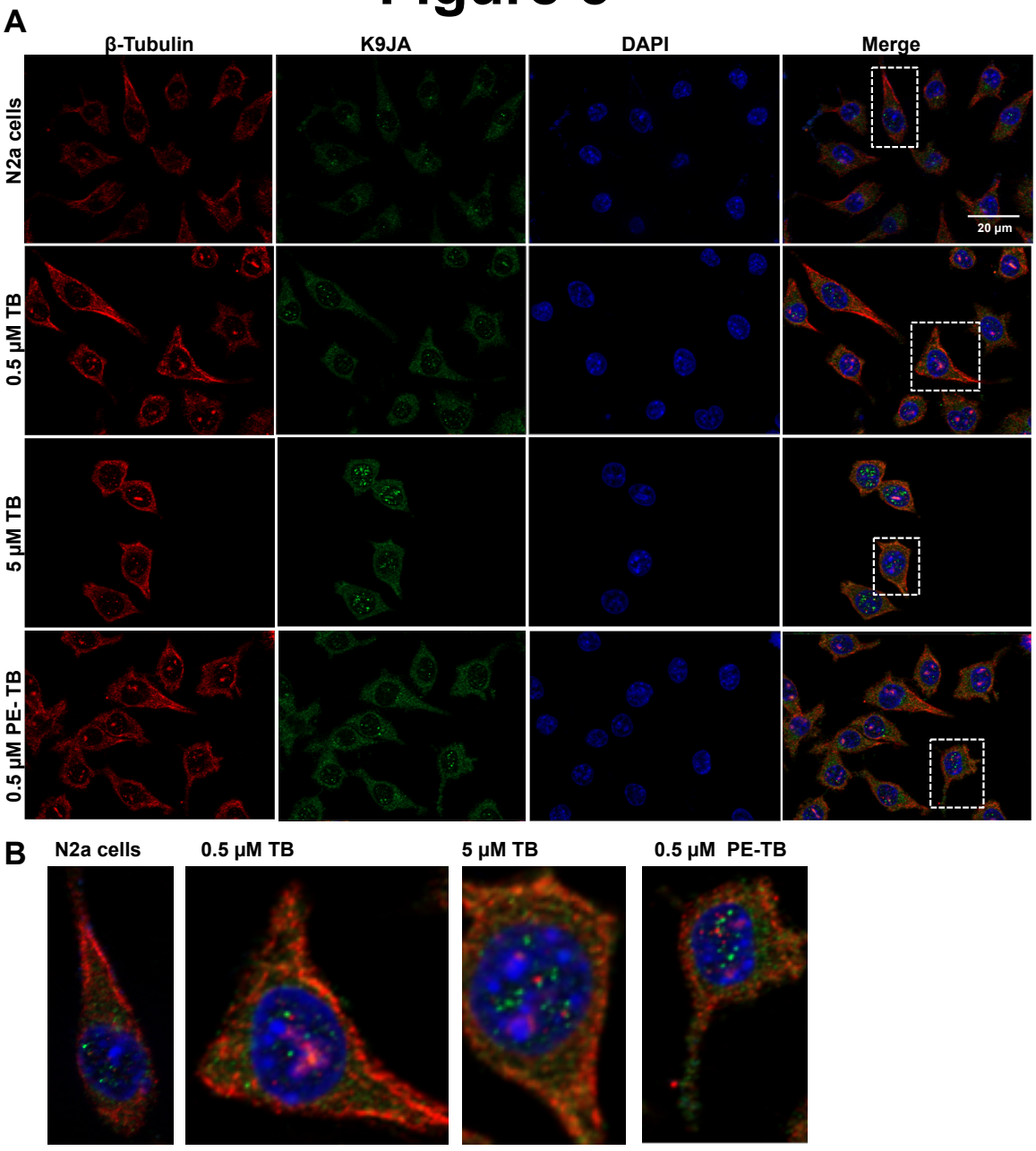
A
β-Tubulin
K9JA
DAPI
Merge
N2a cells
0.5 μM TB
5 μM TB
0.5 μM PE- TB
20 μm
B
N2a cells
0.5 μM TB
5 μM TB
0.5 μM PE-TB

Figure 6

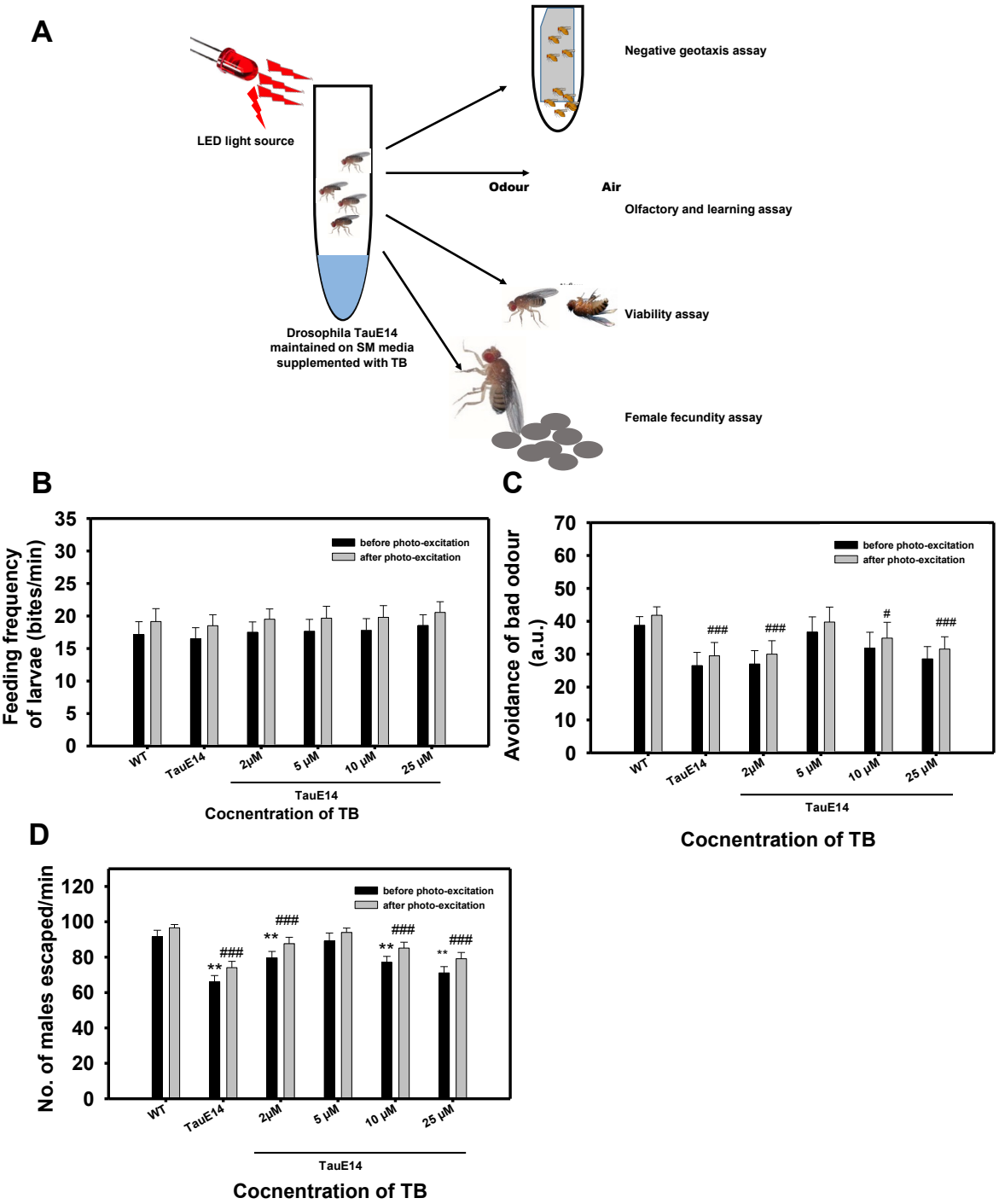
A
LED light source
Negative geotaxis assay
Odour
Air
Olfactory and learning assay
Viability assay
Drosophila TauE14 maintained on SM media supplemented with TB
Female fecundity assay
B
Feeding frequency of larvae (bites/min)
before photo-excitation
after photo-excitation
WT
TauE14
2μM
5 μM
10 μM
25 μM
TauE14
Cocnentration of TB
C
Avoidance of bad odour (a.u.)
before photo-excitation
after photo-excitation
###
#
WT
TauE14
2μM
5 μM
10 μM
25 μM
TauE14
Cocnentration of TB
D
No. of males escaped/min
before photo-excitation
after photo-excitation
**
###
WT
TauE14
2μM
5 μM
10 μM
25 μM
TauE14
Cocnentration of TB

Figure 7

A

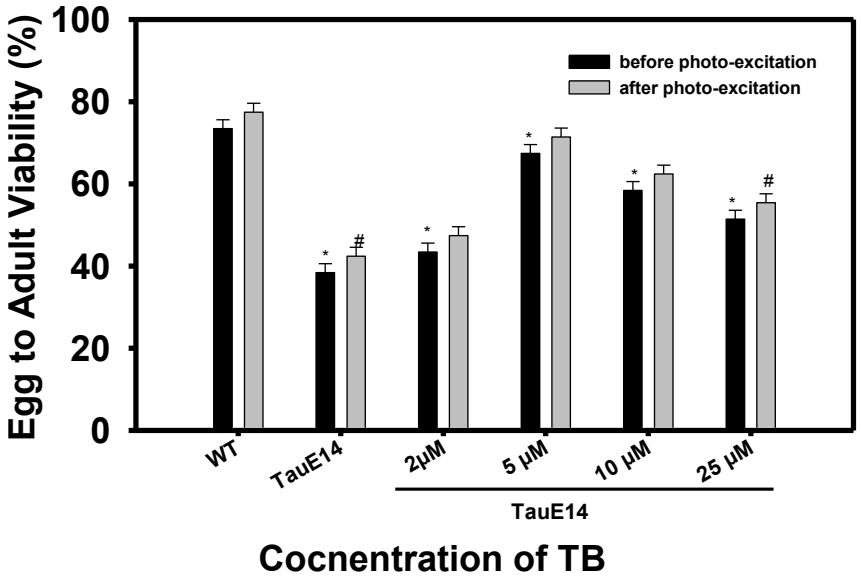
Egg to Adult Viability (%)
100
80
60
40
20
0
before photo-excitation
after photo-excitation
WT
TauE14
2μM
5 μM
10 μM
25 μM
TauE14
Cocnentration of TB

B

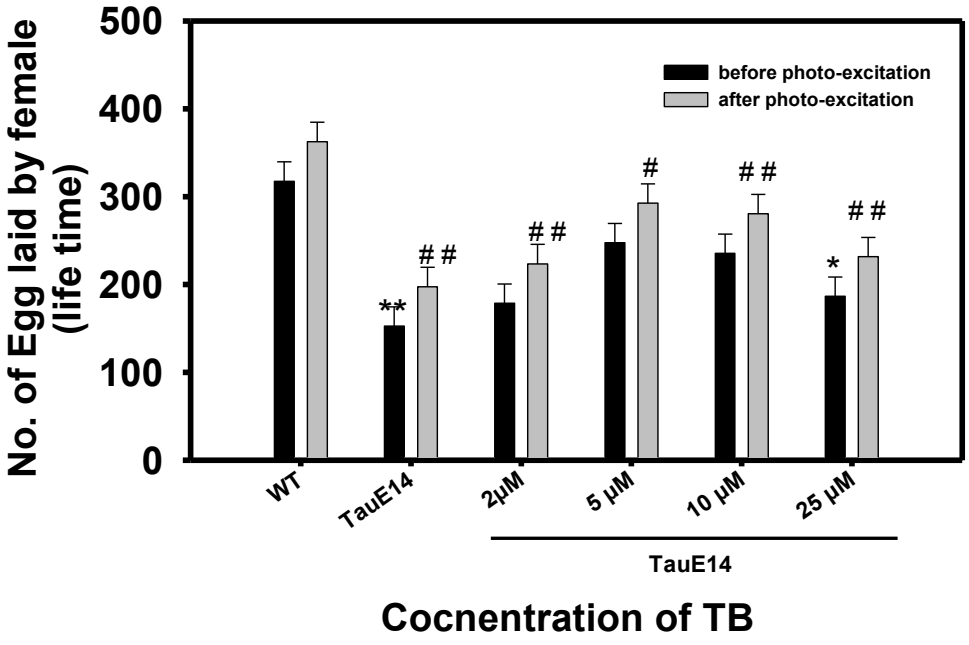
No. of Egg laid by female (life time)
500
400
300
200
100
0
before photo-excitation
after photo-excitation
WT
TauE14
2μM
5 μM
10 μM
25 μM
TauE14
Cocnentration of TB

Figure 8

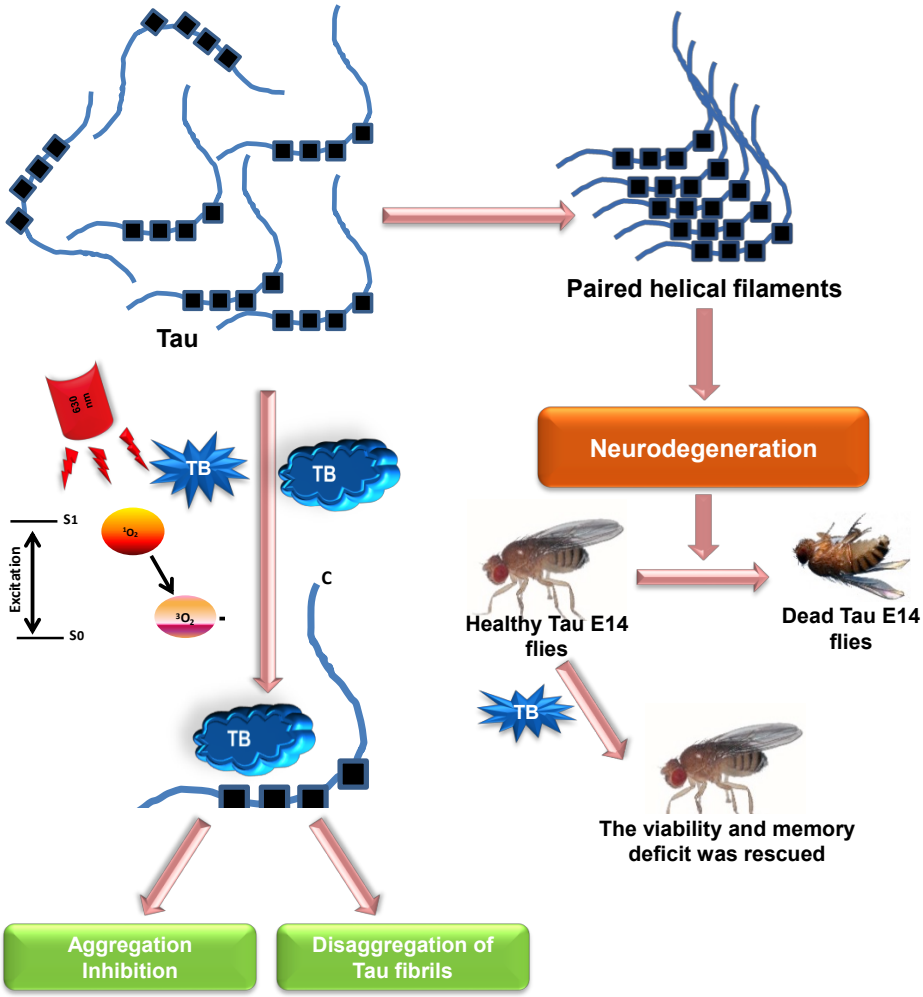
Tau
Paired helical filaments
Neurodegeneration
630 nm
TB
TB
S1
Excitation
S0
$^1O_2$
$^3O_2$
C
TB
Healthy Tau E14 flies
Dead Tau E14 flies
TB
The viability and memory deficit was rescued
Aggregation Inhibition
Disaggregation of Tau fibrils